

Design of Fatigue Resistant Aero Engine Disks

STRAIN POSAVLJAK
 "ORAO" a.d.
 Sabackih djaka bb, 76300 Bijeljina
 BOSNIA AND HERZEGOVINA

STEVAN MAKSIMOVIC
 Military Technical Institute
 Ratka Resanovica 1, 11000 Belgrade
 SERBIA

Abstract: - This paper is partly devoted to problem of holes on aero engine disks. Flat disks with four, six and eight eccentric arranged holes were observed. Estimation of their low cycle fatigue life was performed in conditions of variable revolutions per minute. During that, blocks of variable revolutions per minute of low pressure compressor rotor of one aero engine, were used. Four blocks regulated for ground testing and one block registered during specific training flight. It is shown how an how much low cycle fatigue of disks is dependent of assigned geometry and material nominated for workmanship. Besides that, it is shown how the solution of simple problems can be useful for design of fatigue resistant aero engine disks.

Key-Words: - Flat disks, Stress-strain response, Neuber's hyperbola, Estimation of damages, Low cycle fatigue life estimation

1 Introduction

Fatigue resistance of aero engine disks, to a great extent, depends from assigned geometry and material nominated for workmanship [1-3]. Variable centrifugal forces of blades and own centrifugal forces, without or together with variable temperature, provoke their low cycle fatigue (LCF). Very important mission in design process is to give answer on the question, which geometry and which material to select in order to make disks with satisfying LCF life, expressed in start-stop cycles or flight hours.

2 Low Cycle Fatigue Life

Traditional methods of LCF life estimation of aero engine disks are based on equivalent testing on test benches, flight testing and exploitation testing. In recent twenty years, great research efforts are connected with experimental and analytical methods [6,7].

Analytical method of LCF life estimation is used in design process of fatigue resistant aero engine disks. It includes load, geometry and material data processing.

Design flow chart of fatigue resistant aero engine disks is presented in Fig. 1 and in general, it can be

applied for design all metallic parts subjected to LCF.

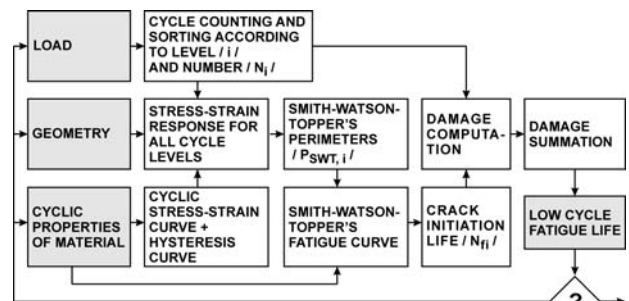


Fig. 1 Design flow chart of fatigue resistant aero engine disks [1]

At first of design process it is necessary to notice and solve simple problems useful for design of fatigue resistant aero engine disks. This time, attention is devoted to problem of holes on disks.

Holes on aero engine disks have important role. They lighten disks and serve for assembling and air cooling.

Some of aircraft accidents were caused by disk fractures, because the disk fractures were initiated in hole areas. One example is given in [1].

3 Case of Flat Disks with Eccentric Arranged Holes

3.1 Geometry and loads

Useful conclusions needed for make of decisions in connection with size, number and arrangement of holes on aero engine disks, designer can draw by analysis of flat disks with eccentric arranged holes, taking in account results of LCF life estimation. Flat disks with 4, 6 an 8 eccentric arranged holes (Fig. 2) were served here as an example. Their LCF life estimation was carried out in conditions of variable revolutions per minute (R.P.M).

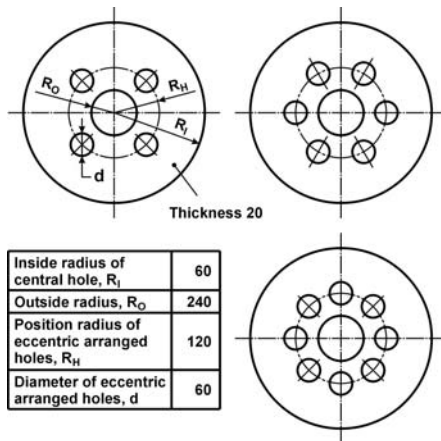


Fig. 2 Geometry definition of flat disks with 4, 6 and 8 eccentric arranged holes

Variable R.P.M was simulated using R.P.M blocks of low pressure compressor rotor of one aero engine (Fig. 3). Blocks A, B, C and D are regulated and serve for ground engine testing. Block E was registered during specific training flight.

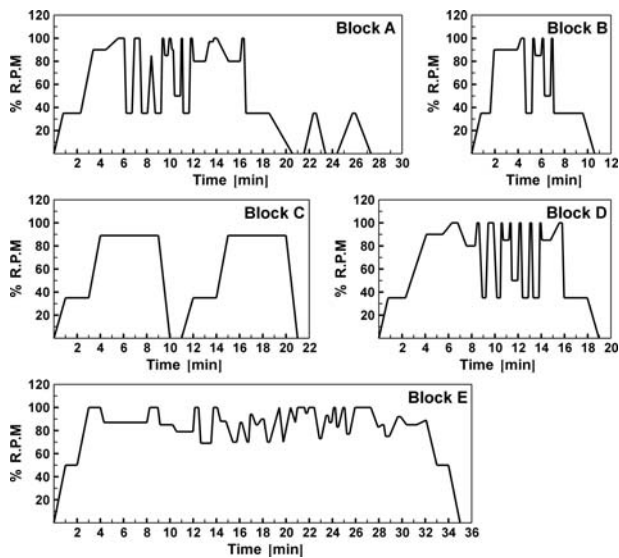


Fig. 3 Blocks of variable R.P.M of low pressure compressor rotor of one aero engine [1]

In order to estimate LCF life, listed blocks were decomposed in simple X-Y-X R.P.M cycles. For example, decomposition of block D, according to recommendations from [2] is shown in Fig. 4.

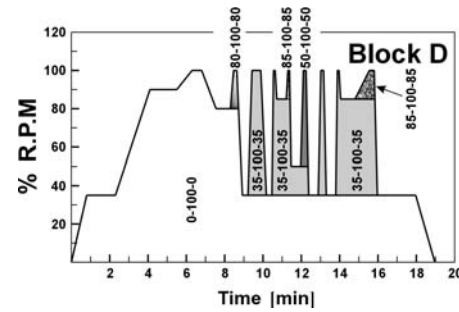


Fig. 4 Block D decomposed on simple R.P.M cycles

Simple X-Y-X R.P.M cycles per blocks, sorted according to level / i / and number / N_i /, are contained in Tables 1-5.

Table 1 X-Y-X R.P.M Cycles in block A

i	X-Y-X R.P.M Cycle	N_i
1	0-100-0	1
2	35-100-35	3
3	35-85-35	1
4	50-100-50	1
5	80-100-80	2
$k = 6$	85-100-85	1

Table 2 X-Y-X R.P.M Cycles in block B

i	X-Y-X R.P.M Cycle	N_i
1	0-100-0	1
2	35-100-35	1
3	50-100-50	1
$k = 4$	85-100-85	1

Table 3 X-Y-X R.P.M Cycles in block C

i	X-Y-X R.P.M Cycle	N_i
$k = 1$	0-89-0	2

Table 4 X-Y-X R.P.M Cycles in block D

i	X-Y-X R.P.M Cycle	N_i
1	0-100-0	1
2	35-100-35	4
3	50-100-50	1
4	80-100-80	1
$k = 5$	85-100-85	2

Table 5 X-Y-X R.P.M Cycles in block E

i	X-Y-X R.P.M Cycle	N _i
1	0-100-0	1
2	70-100-70	3
3	70-87-70	1
4	70-94-70	1
5	73-100-73	1
6	75-92-75	1
7	77-100-77	1
8	79-100-79	1
19	83-100-83	1
10	83-85-83	1
11	85-89-85	1
12	85-90-85	1
13	87-100-87	3
k = 14	95-100-95	1

3.2 Cyclic Properties of Material

Assume that material nominated for workmanship of disks in Fig. 2 is steel 13H11N2V2MF in state S1 (State of delivery) and in state S2 (Quenched and tempered state: Heating at 1000 °C, Quenching in oil, Tempering at 640 °C, Air cooling). Cyclic properties of this steel are contained in Table 6.

In dependence of named steel states, flat disks with 4, 6 an 8 eccentric arranged holes, bring marks: D4S1, D6S1, D8S1 and D4S2, D6S2 and D8S2.

Table 6 Cyclic properties of steel 13H11N2V2MF

PROPERTY	STATE	
	S1	S2
Modulus of elasticity, E [MPa]	206682	229184.6
Cyclic strength coefficient, K' [MPa]	1103	1140
Cyclic strain hardening exponent, n'	0.118	0.0579
Fatigue strength coefficient, σ'_f [MPa]	1818.8	1557.3
Fatigue strength exponent, b	-0.144	-0.0851
Fatigue ductility coefficient, ϵ'_f	0.5351	0.3175
Fatigue ductility exponent, c	-0.6619	-0.7214

Cyclic properties of steel 13H11N2V2MF in state S1 were taken from [3] while cyclic properties of the same steel in state S2 are result of project which is in progress.

3.3 Stress-Strain Response

Stress response of disks D4S1, D6S1, D8S1 and DS1, for maximum number of R.P.M = 11860, was obtained using the finite element method (FEM) implemented in NASTRAN software. Distribution of principal stresses σ_1 of listed disks is presented in Fig. 5. All disks were observed as ideal elastic circular plates.

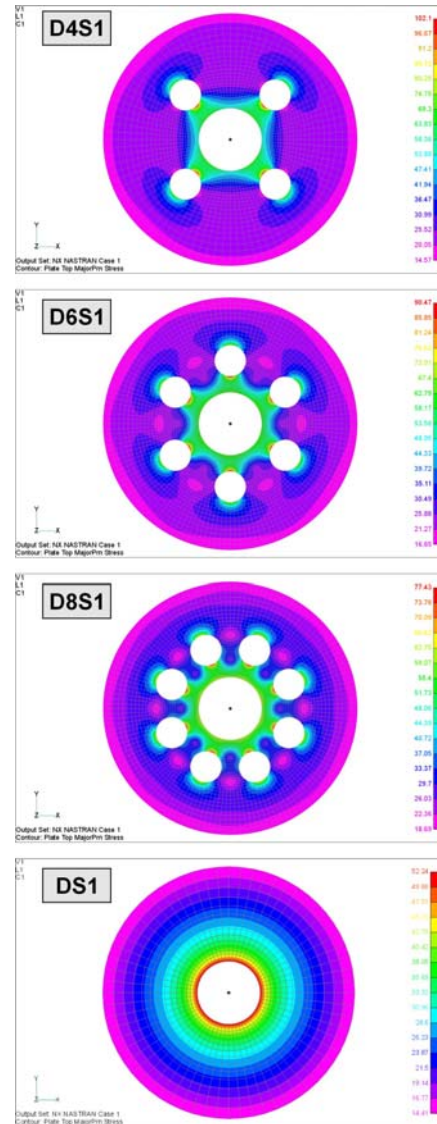


Fig. 5 Distribution of principal stresses σ_1 on disks D4S1, D6S1, D8S1 and DS1

Principal stresses σ_1 have maximum values at critical points P (Fig. 6):

$$\begin{aligned} \sigma_{1,P}(\text{D4S1}) &= 1021.0 \text{ MPa,} \\ \sigma_{1,P}(\text{D6S1}) &= 904.7 \text{ MPa} \\ \sigma_{1,P}(\text{D8S1}) &= 774.3 \text{ MPa.} \end{aligned}$$

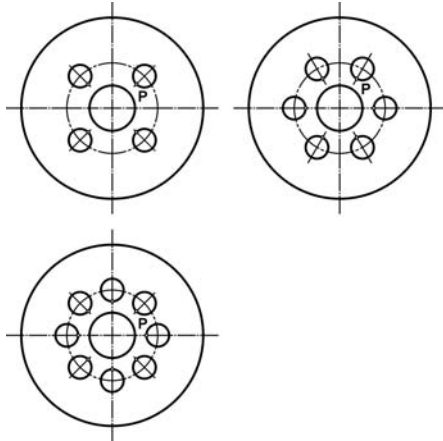


Fig. 6 Position of critical points P on flat disks with eccentric arranged holes

Position radius of critical points P is $R = 90$ mm. For that radius, value of principal stress σ_1 on disk DS1, amounts:

$$\sigma_{1,R90} (DS1) = 358.3 \text{ MPa.}$$

If suppose that upper stress is nominal stress (σ_n), than stress concentration factor K_{TP} for critical points P of disks with 4, 6 and 8 eccentric arranged holes (disks D4, D6 and D8) can be determined by expression

$$K_{TP} = \frac{\sigma_{1,P}}{\sigma_n} \tag{1}$$

Stress concentration factors for critical points P of disks D4, D6 and D8 according to (1) have next values:

$$\begin{aligned} K_{TP} (D4) &= 2.849, \\ K_{TP} (D6) &= 2.525, \\ K_{TP} (D8) &= 2.161. \end{aligned}$$

Real Stress-strain response of disks in Fig. 2, in comparison with stress-strain response of disks as ideal elastic circular plates is completely different. Namely, their stress-strain response can be described by hysteresis loops associated to all simple X-Y-X R.P.M cycles in Tables 1-5.

Upper point of hystereses loops was obtained by solution of system equations

$$\begin{aligned} \sigma \varepsilon &= \frac{K_f^2 \sigma_n^2}{E} \\ \varepsilon &= \frac{\sigma}{E} + \left(\frac{\sigma}{K'} \right)^{\frac{1}{n'}} \end{aligned} \tag{2}$$

Widths and heights of hystereses loops were obtained by solution of system equations

$$\begin{aligned} \Delta \sigma \Delta \varepsilon &= \frac{K_f^2 (\Delta \sigma_n)^2}{E} \\ \Delta \varepsilon &= \frac{\Delta \sigma}{E} + 2 \left(\frac{\Delta \sigma}{2K'} \right)^{\frac{1}{n'}} \end{aligned} \tag{3}$$

The first equations in (2,3) are two forms of Neuber's hyperbola. The second equation in (2) is equation of cyclic stress-strain curve. The second equation in (3) is equation of hysteresis curve [4,5].

Systems (2,3) were solved graphical using DRAFTING module of I-DEAS software. By special Visual FORTRAN programs, Neuber's hyperbolas, cyclic stress-strain curves and hysteresis curves, were copied in corresponding spline curves.

Example of graphical stress-strain response of disks D4S1 and D4S2, for the basic 0-100-0 R.P.M cycle, obtained by solution of systems (2,3), is given in Fig. 7.

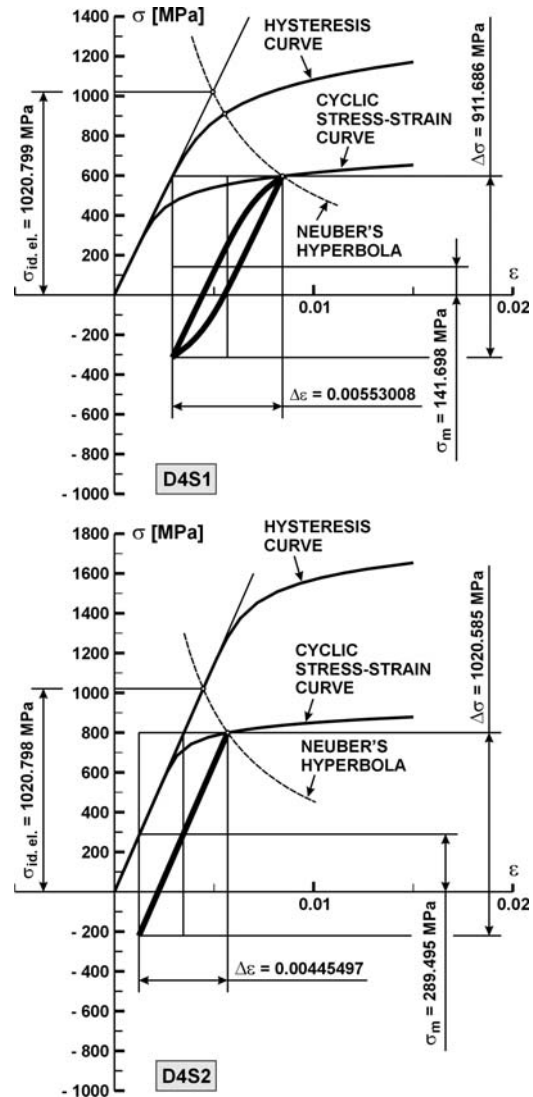


Fig 7 Stress-strain response of disks D4S1 and D4S2 for the basic 0-100-0 R.P.M cycle

Notch factor K_f in systems (2,3) is conditional equalized with stress concentration factors K_{TP} , connected with critical points P of disks in Fig. 2.

Values of nominal stresses σ_n and ranges $\Delta\sigma_n$ of these stresses, needed for solution of systems (2,3), for all levels of X-Y-X R.P.M cycles in Tables 1-5, were calculated using expressions

$$\sigma_{ni} = 358.3 \left(\frac{Y_i}{100} \right)^2$$

$$\Delta\sigma_{ni} = 358.3 \left[\left(\frac{Y_i}{100} \right)^2 - \left(\frac{X_i}{100} \right)^2 \right] \tag{4}$$

3.4 Estimation of Damages

Estimation of damages D per blocks of variable R.P.M, were carried out using Kurath’s expression [6] in form

$$D = \sum_{i=1}^k \frac{N_i}{N_{fi}} \left(\frac{\Delta\sigma_i}{\Delta\sigma_h} \right)^{\frac{1}{d}} \tag{5}$$

where d is interactive exponent, and $\Delta\sigma_h$ is highest range of stress response in corresponding block of variable R.P.M.

Expression for determination of interactive exponent d has next form

$$d = \frac{b}{b + c + 1} \tag{6}$$

where b and c are exponents in Table 6.

Numbers N_i of X-Y-X R.P.M cycles were taken from Table 6, while numbers N_{fi} were determined using Smith-Watson-Topper’s fatigue curves given in general form

$$P_{SWT} = \sqrt{\sigma_{max} \frac{\Delta\epsilon}{2} E} = \sqrt{(\sigma'_f)^2 (N_f)^{2b} + E\sigma'_f \epsilon'_f (N_f)^{b+c}} \tag{7}$$

and Smith-Watson-Topper’s perimeters

$$P_{SWT,i} = \sqrt{\sigma_{max,i} \frac{\Delta\epsilon_i}{2} E} \tag{8}$$

Graphical illustration of Smith-Watson-Topper’s fatigue curves of steel 13H11N2V2MF in state S1 and S2, copied in spline curves, is shown in Fig. 8.

Damages data (D_A , D_B , D_C , D_D and D_E) per blocks A, B, C, D and E in Fig. 3 are included in Table 7.

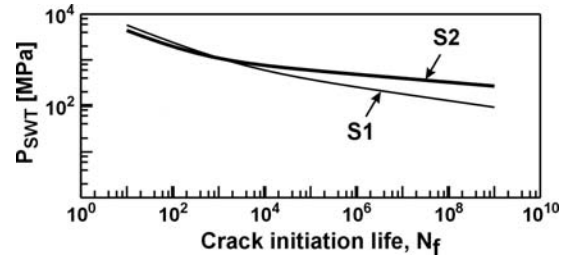


Fig. 8 Smith-Watson-Topper’s fatigue curves of steel 13H11N2V2MF in state S1 and S2

Table 7. Damages data per blocks A, B, C, D and E of variable R.P.M

	Disk	
	D4S1	D4S2
D_A	0.000427123172	0.000078268303
D_B	0.000225400288	0.000045341240
D_C	0.000077417357	0.000008398562
D_D	0.000462566650	0.000090398462
D_E	0.000325351888	0.000034526673
	D6S1	D6S2
D_A	0.000280163718	0.000034081173
D_B	0.000147241554	0.000020027307
D_C	0.000049074937	0.000002946159
D_D	0.000303029075	0.000039698583
D_E	0.000214619927	0.000015002976
	D8S1	D8S2
D_A	0.000160034768	0.000010041081
D_B	0.000084180653	0.000005977596
D_C	0.000026695854	0.000000573599
D_D	0.000173887629	0.000011781688
D_E	0.000120135609	0.000004416540

3.5 Low Cycle Fatigue Life Estimation

Four hundred flight hours of overhaul intermediate time of aero engine which interesting here, is consisted of: 2 blocks A, 400 blocks B, 15 blocks C, 14 blocks D, and approximately 685 blocks E of variable R.P.M [1].

With upper fact, total damage for 400 flight hours of overhaul intermediate time, was determined by expression

$$D_T = 2D_A + 400D_B + 15D_C + 14D_D + 685D_E \tag{9}$$

Damages D_{1h} per one flight hour were determined using expression

$$D_{1h} = \frac{D_T}{400} \quad (10)$$

Low cycle fatigue life expressed in flight hours is reciprocal value of D_{1h} .

Total damages, damages per one flight hour, and LCF life (LCFL) data, of discussed flat disks, are contained in Table 8. Histogram of LCFL data is presented in Fig. 9.

Table 8 Damages and LCFL data of discussed flat disks

Disk D4S1	
D_T	0.321517598279
D_{1h}	0.000803793996
LCFL [h]	1244
Disk D4S2	
D_T	0.043335360509
D_{1h}	0.000108338401
LCFL [h]	9230
Disk D6S1	
D_T	0.211450130136
D_{1h}	0.000528625325
LCFL [h]	1891
Disk D6S2	
D_T	0.018956096253
D_{1h}	0.000047390241
LCFL [h]	21101
Disk D8S1	
D_T	0.119120087517
D_{1h}	0.000297800219
LCFL [h]	3357
Disk D8S2	
D_T	0.005609998079
D_{1h}	0.000014024995
LCFL [h]	71301

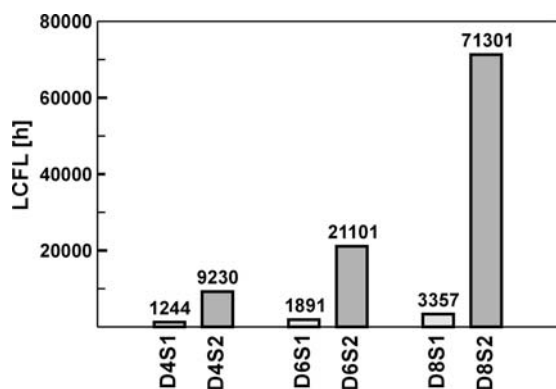


Fig 9 Histogram of LCFL data

4 Conclusion

This study combined finite element structural analysis with strain-life equations to develop a simple and effective procedure for the fatigue crack initiation life of aero engine disks. The Neuber method is used to estimate elastic-plastic stresses and strains at the roots of notches on the basis of elastic stress analysis. It applies where the yielding is limited in extent; under these circumstances it provides a reasonable approximation for the redistribution of stress and strain.

By solution of simple problem of flat disks with four, six and eight eccentric arranged holes, it is shown how and how much number of holes can influence on low cycle fatigue life of aero engine disks. However, influence of material, selected for workmanship is more essential. Results of low cycle fatigue life show that aero engine disks with 4 and 6 eccentric arranged holes in design process it is necessary to avoid.

References:

- [1] S. Posavljak, S. Maksimovic, Design of Aero Engine Disks on Fatigue Life, *Proceedings of Scientific-Expert Meeting IRMES '06*, pp 379-386, University of Banja Luka, Mechanical Faculty, 2006 (in Serbian)
- [2] V. I. Demyanushko, I. A. Birger, *Strength Calculation of Rotating Disks*, Moscow, Mashinostroenie, 1978 (in Russian)
- [3] S. Posavljak, *Stress-Strain Analysis and Fatigue of Materials of Turbojet Engine Rotating Disks*, Master thesis, Belgrade University, Mechanical faculty, 1999 (in Serbian)
- [4] A. J. Bannantine, J. Comer, J. Handrock, *Fundamentals of Material Fatigue Analysis*, Prentice-Hall, Englewood Cliffs, New Jersey 1990
- [5] M. D. Jankovic, *Low Cycle Fatigue*, Belgrade University, Mechanical faculty, 2001 (in Serbian)
- [6] A. Fatemi, L. Yang, Cumulative fatigue damage and prediction theories: a survey of the state of the art for homogeneous materials, *International Journal of Fatigue*, Vol. 20, No. 1, 1998, pp. 9-34.
- [7] S. Maksimovic, Fatigue Life Analysis of Aircraft Structural Components, *Scientific Technical Review*, Vol. LV, No.1, 2005.